



Imaging through dynamical scattering media by two-photon absorption detectors

WEI LIU,¹ ZHIHAO ZHOU,²  LEI CHEN,¹  XIN LUO,²  YUEHAN LIU,³ XIANFENG CHEN,^{1,4} AND WENJIE WAN^{1,2,*} 

¹The State Key Laboratory of Advanced Optical Communication Systems and Networks, School of Physics and Astronomy, Shanghai Jiao Tong University, Shanghai 200240, China

²MOE Key Laboratory for Laser Plasmas and Collaborative Innovation Center of IFSA, University of Michigan-Shanghai Jiao Tong University Joint Institute, Shanghai Jiao Tong University, Shanghai 200240, China

³Whiting School of Engineering, Johns Hopkins University, Baltimore, MD 21218, USA

⁴Collaborative Innovation Center of Light Manipulation and Applications, Shandong Normal University, Jinan 250358, China

*wenjie.wan@sjtu.edu.cn

Abstract: Imaging through a dynamical opaque scattering medium is an almost impossible task, where strong multiple light scattering from moving scatters dynamically prevents imaging formations even with state-of-art techniques like correlation imaging or adaptive optics. Meanwhile, a small number of ballistic photons can still penetrate through but require demanding detection in terms of a ultrashort time gate and high sensitivity. However, visible light is strongly scattered for most of scattering media. Here we experimentally demonstrate a non-invasive coherent imaging scheme based on two-photon absorption capable of imaging through dynamical scattering media with a length equivalent to 28 times mean free paths for single photon transport, where two-photon absorption in a conventional semiconductor photodetector when phase matching is not required works over a wide bandwidth so it can support a fast time gate down to femtosecond level, short enough to distinguish ballistic photons from scattering background, and allows accessing longer wavelengths for deeper penetration. This technique combined with successful optical coherence tomography may pave a new way for imaging through fog, storm, and rain as well as biomedical imaging applications.

© 2021 Optical Society of America under the terms of the [OSA Open Access Publishing Agreement](#)

1. Introduction

Imaging through scattering media, a long-standing problem, is among the biggest challenges with a common physical root cause [1] in many fields including biomedical optical imaging [2], microwave radar [3], seismic wave in oil exploration [4] and electronic wave in the condensed matter [5], where multiple wave scattering from random complex samples induces strong imaging distortion and limits penetration depth in the same time. Recently, pioneering experiments to tackle this problem have been demonstrated with the help of memory effect [6,7], phase conjugation [8], and the scattering matrix inversion [9]. However, these methods require initial recording prior knowledge about scattering medium for imaging purposes; other adaptive approaches [10,11] undergo time-consuming wavefront shaping processes to construct a “scattering lens”. These factors halt practical imaging applications beyond stationary scattering medium, e.g. imaging through dynamical scattering medium like fog, sandstorms, air turbulence, and live bio-samples. Recent attempts utilizing speckle correlations with complex numerical reconstructions [12,13] seems to overcome this limitation, but requiring back-illumination sources, which are still not as ideal as non-invasive imaging mode in a reflective configuration [14].

On the other hand, ballistic imaging has proven itself a successful approach for imaging through scattering layers by distinguishing ballistic photons from their strong scattering background [15].

Previously, it is possible to form sharp images through a weak scattering media using a coherent gate of optical coherence tomography (OCT) [16] in a non-invasive reflective configuration. However, this method is an inherent phase-dependent process, making it impossible to image through a dynamic environment. For much strong scattering, ballistic imaging can only be obtained with fine time-resolved techniques to pick up extremely weak ballistic photons, e.g. Kerr gate [15], time-gated imaging [17]. However, the difficult nonlinear optical setup in the Kerr gate and low-temporal resolution of electronic time-gated imaging greatly limit their practical applications. Recently, the photon bunching effect based on two-photon absorption has exhibited ultrashort temporal resolution down to the femtosecond level with a conventional semiconductor photodetector [18], extendable to a CMOS array [19], immediately opening a new way for ballistic imaging. As compared to one-photon OCT, two-photon OCT can be realized with second-order photon correlation, i.e. intensity, which is phase-independent [20]. Furthermore, two-photon processes allow accessing longer wavelengths for deeper penetration [21,22] in the bandwidth-limited semiconductor photodetectors. Both of the two features combine for an ideal new platform for ballistic imaging through a scattering medium, which may enable distortion-free imaging from dynamical scattering background.

In this work, we experimentally demonstrate non-invasive coherent imaging through moving scattering media based on two-photon absorption detection. Nonlinear two-photon absorption undergoes an intermediate step in the scale of femtosecond during a cascaded two-photon process, which is utilized directly as a time gate for ultrafast measurement. This ultrafast coherent time-gate detection can temporally distinguish ballistic photons from their strong scattering background offering a unique tool for ballistic imaging through scattering media. Under this framework, two configurations of self-referenced imaging and another one with an ultrafast time-gate reference are realized for scanned ballistic imaging over a thickness of 28 times mean free paths using a single conventional semiconductor photodetector. Furthermore, such two-photon coherent imaging by TPA exhibits strong resistance against moving scattering media due to the nature of light's ballistic transportation. These results open up new avenues for their practical applications in biomedical imaging and imaging through dynamical scattering environments.

2. Method

2.1. Ballistic and scattering photon detection by two-photon absorption

Hidden objects behind scattering layers cannot be directly resolved through conventional imaging techniques due to the strong scattered light. However, only a small portion of photons ahead of others travel undisturbedly in a straight ballistic fashion, while most photons are lagging, suffering from random scattering multiple times as shown in Fig. 1. However, these ballistic photons are hard to catch due to ultrashort time duration difference (\sim femtosecond level depending on the scattering thickness) compared to the majority, i.e. scattering photons. Previously, coherent gating in one photon OCT can allow coherent detections of these photons using ultrawide spectrum source, i.e. ultrashort coherence time [23], but this method is limited by the dynamical phase perturbations from the medium [20]. Meanwhile, nonlinear Kerr gate for scattering imaging [24] is complicated with nonlinear optical configuration and very demanding for laser power, methods based on electronic time gate are slow in terms of temporal resolution.

To address this issue, we utilize two-photon absorption in a GaAs photomultiplier tube (PMT) [25] (Hamamatsu, H7421-50), where one photon below the bandgap of GaAs (1.37 eV, 890 nm) can only excite an electron to a virtual state (Fig. 1(a)) with a short lifetime (\sim femtosecond) inverse proportion to bandgap energy [26] if only a second photon with enough photon energy can further pump the electron to the conduction band (Fig. 1(a)). In this manner, TPA serves as an ideal ultrashort time gate, which only depends on input light intensity satisfying second-order intensity correlation [27]. Here we explore this feature by focusing a wideband source with an erbium-doped fiber amplifiers (EDFA) amplified spontaneous emission (ASE) source (centered at

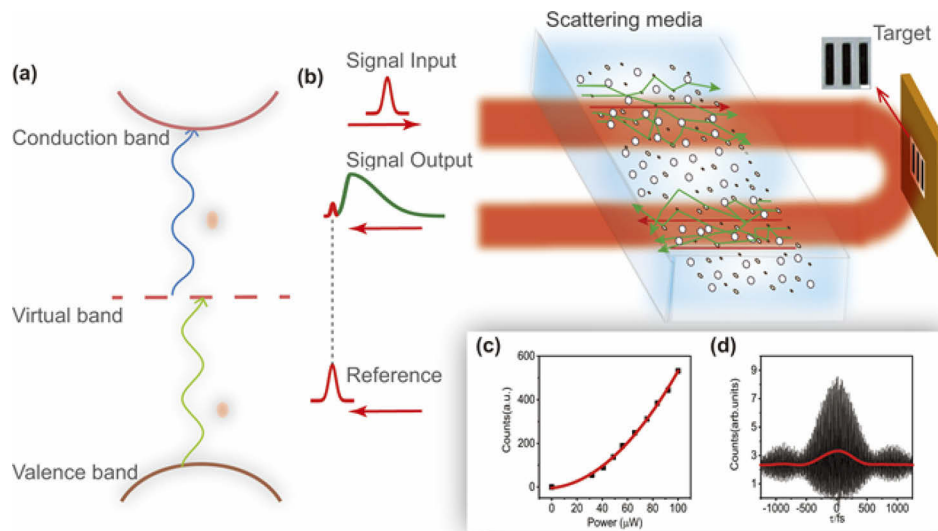


Fig. 1. The principle of coherent imaging through scattering media with two-photon absorption. (a) TPA process in which the valence band absorbs one photon (reference) to a virtual state, subsequently absorbs another photon (signal) to the conduction band, and produces a photocurrent. (b) Incident pulse is strongly scattered through scattering media, reflected by the target, and propagates again through the scattering media, forming a temporal distribution with distinct ballistic and diffusive photon regimes according to their arriving time. (c) TPA signal from the PMT counts exhibits a quadratic dependence on the incident power. (d) Autocorrelation of the TPA signal as a function of the delay τ in the Michelson interferometer with an EDFA source. The scale bar $500\mu\text{m}$

$1.5\ \mu\text{m}$ wavelength) to the PMT, observing quadratic growth of TPA signals when increasing input power in Fig. 1(c). With a Michelson interferometer, we examine such an ultrashort time gate to be $\sim 500\text{fs}$ FWHM in its autocorrelation function, which is short enough to distinguish ballistic light from scattering background in the following experiment. This time gate can be further reduced to $\sim 50\text{fs}$ with a broadband supercontinuum source discussed (bandwidth $\sim 150\text{nm}$), which may be helpful for a thin scattering medium.

Figure 2 demonstrates TPA's unique feature of ultrafast time gate capable of catching ballistic light through scattering media. Experimentally, a standard Michelson interferometer is modified with an additional scattering layer (soymilk with a diffusion length of 2mm) placed in one of the arms. The light source is a broadband supercontinuum source. In this configuration, a reference beam with a tunable delay is scanned longitudinally and interfered with the signal light reflected by a target mirror through the scattering layer. In this non-invasive reflective manner, we can retrace the reflected temporal signal including both scattering and ballistic light in Fig. 2(b). The temporal difference between ballistic photons and diffusive photons is determined by the scattering ability of scattering media. At first glance, it seems TPA reflected signal hump lasts over 2 picosecond time duration with no clear boundary between the ballistic photons and the scattered one. But if we zoom in this time trace and compare the portion of signals near zero-time delay, i.e. two arms with the same length, and others, a clear temporal oscillation pattern (Fig. 2(b)) is pronounced indicating the interference effect between the two arms. The interference arises from coherent ballistic photons and the reference, while scattered photons lost such coherence due to multiple scattering processes. This gives us a tool to separate the ballistic

components from the rest. Later, combined with an averaging and envelope algorithm [16], we proceed to utilize this method to construct images behind scattering layers.

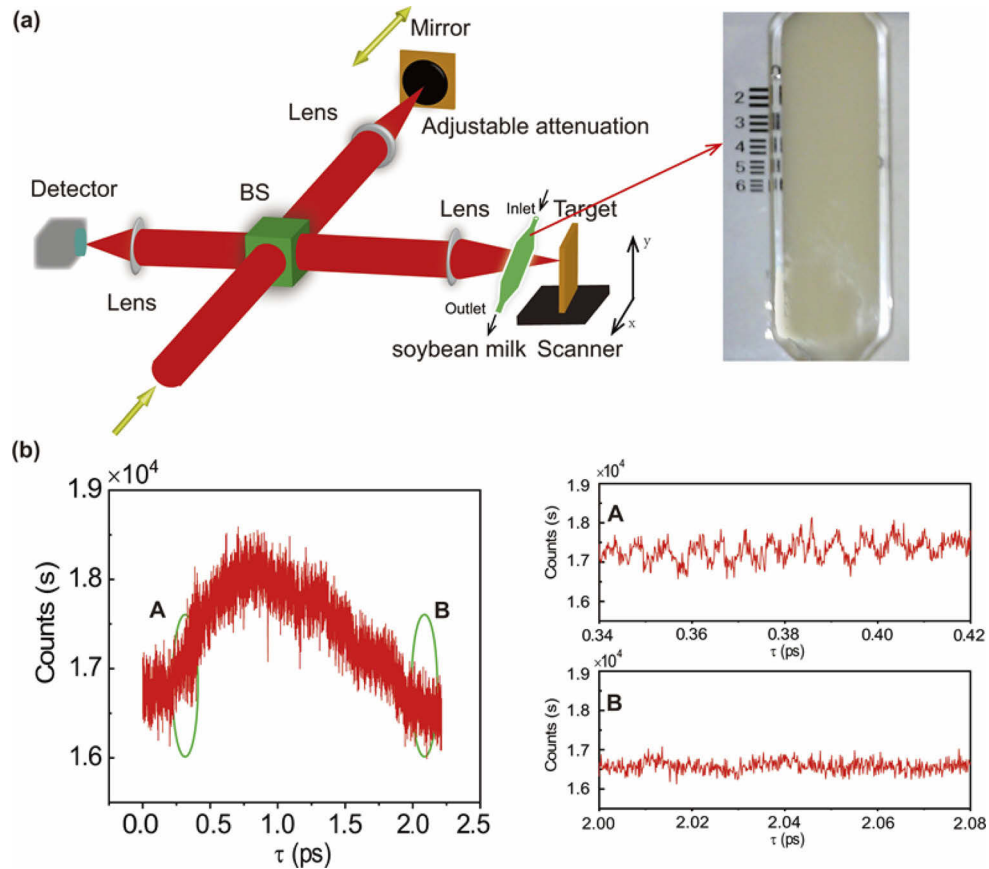


Fig. 2. Temporal distributions of photon transmission through scattering media using an ultrafast TPA time gate. (a) A Michelson interferometer with two symmetric lens-mirror reflected arms for time-delayed measurement of TPA. A cuvette flowed by strong scattering soymilk is placed on the imaging arm. Lens: 100mm, BS: beam splitter, Objective lens: 20X, Detector: GaAs photomultiplier tube. Broadband source: supercontinuum source. All of the experiments are carried out in a photon-proof box. (b) Temporal distributions of the incident pulse through scattering media. (A) Zoom-in temporal trace around point A shows an interference pattern between the reference beam and ballistic photons. (B) Zoom-in temporal trace around point B shows phase-independent counts without interferences from diffusive photons.

2.2. Theory of TPA based two-photon OCT

This configuration in Fig. 2(a) also resembles the traditional one-photon OCT technique, effectively creating a two-photon OCT version by replacing a one-photon detector with a TPA detector [20]. As compared with one-photon OCT depending on the first-order correlation (electrical field including phase), such two-photon OCT is intensity-correlated [20], offering a unique feature of phase-insensitive detection through dynamical turbulence [20]. Theoretically, this intriguing

result can be understood by comparing the coherence functions for both cases [18,28]:

$$S^{(1)}(\tau) = \left[1 + \frac{2\sqrt{I_1 I_2}}{I_1 + I_2} \text{Re}(e^{-i\omega\tau}) \right] \times (I_1 + I_2) \quad (1)$$

$$S^{(2)}(\tau) = \{1 + 2G_2(\tau) + \text{Re}[F_2(\tau)e^{-2i\omega\tau}] + 4\text{Re}[F_1(\tau)e^{-i\omega\tau}]\} \times (I_1 + I_2) \quad (2)$$

$$\tilde{S}(\tau) = \int_{x_0}^{x_1} \int_{y_0}^{y_1} \int_0^T S(\tau - \Delta t(x, y, t)) dx dy dt \quad (3)$$

where τ is the delay time between the two interference arms with intensities, I_1 and I_2 . $G_2(\tau)$ is the intensity autocorrelation function, while F_1 and F_2 are the phase interferograms at the central frequency ω and 2ω , respectively. Obviously, $S^{(2)}(\tau)$ associated with two-photon OCT can exhibit a zero-delay peak signal, 8 times of its background with a large τ , in contrast, $S^{(1)}(\tau)$ indicates a maximum peak-to-background ratio of 2:1, much smaller than the two-photon case, which gives two-photon OCT an edge over its one-photon counterpart in terms of signal-to-noise ratio (SNR) for imaging, more discussions on light sources and their SNR can be found in Ref. [20]. More importantly, both cases in real imaging applications are highly sensitive to the relative phase variations between the two reference arms, directly manifested in the phase terms in $S^{(1)}(\tau)$ and $S^{(2)}(\tau)$, where $S^{(1)}(\tau)$ reveals a first-order interference beating at ω , while $S^{(2)}(\tau)$ shows an additional second-order interference at 2ω due to the TPA. Explicitly, the influence of external phase variations can be revealed in a temporal averaging function in Eq. (3), which integrates over $S^{(1)}(\tau)$ or $S^{(2)}(\tau)$ within a timeframe T , leading to a phase smearing and consequently reduce the SNR. As a result, the peak value of $S^{(1)}(0)$ will reduce to the same value, i.e. 1, as its background, in contrast, $S^{(2)}(0)$ only retract to 2, preserving the signal despite the phase variations. This paves the way for two-photon OCT imaging in some complex and dynamic environments.

3. Results

3.1. Comparison of one-photon and two-photon OCTs through dynamical scattering media

To verify this theory, we experimentally perform two separated experiments to compare one-photon and two-photon OCTs through a turbulent and rapid phase-varying opaque medium. Using the same experimental apparatus in Fig. 2(a) with flowing soymilk through the cuvette, the one-photon OCT is realized using an ASE source with ~5mW input power and center wavelength at 1064nm detected by an avalanche photodiode, while the two-photon OCT is implemented using ASE source with ~80mW input power and center wavelength at 1550nm detected by the aforementioned PMT. The opaque scattering soymilk is externally pumped to flow inside the cuvette with a controllable flowing speed. As shown in Fig. 3(a), we indeed observe the degradation of signal amplitudes comparing the stationary and the flowing cases for both scenarios. The signal amplitudes measured by the visibility from Fig. 3(a) decline with the increasing flow velocity for both cases in Fig. 3(b). However, two-photon OCT is hardly affected by the moving scatters, only dropping around 7% at the velocity of 0.13m/s from its stationary peak value. In comparison, one-photon case drastically reduces by 30% during the same process. Clearly, this indicates the phase-insensitive nature of two-photon OCT based on TPA, which may be beneficial for dynamical scattering imaging. Furthermore, we conduct another contrast experiment to compare the penetration capability of the two imaging methods. Here the concentration of soymilk powder in the solution is gradually increased to enhance the scattering property, the corresponding maximum optical path length is measured to be 8/18 (thickness)times of scattering mean free path for 1550nm/1064nm light, respectively. We observe

a 90% signal drop for the two-photon OCT, while over 99% signal drop for the one-photon case. In this aspect, two-photon OCT may outperform its one-photon counterpart for deeper penetration in imaging applications.

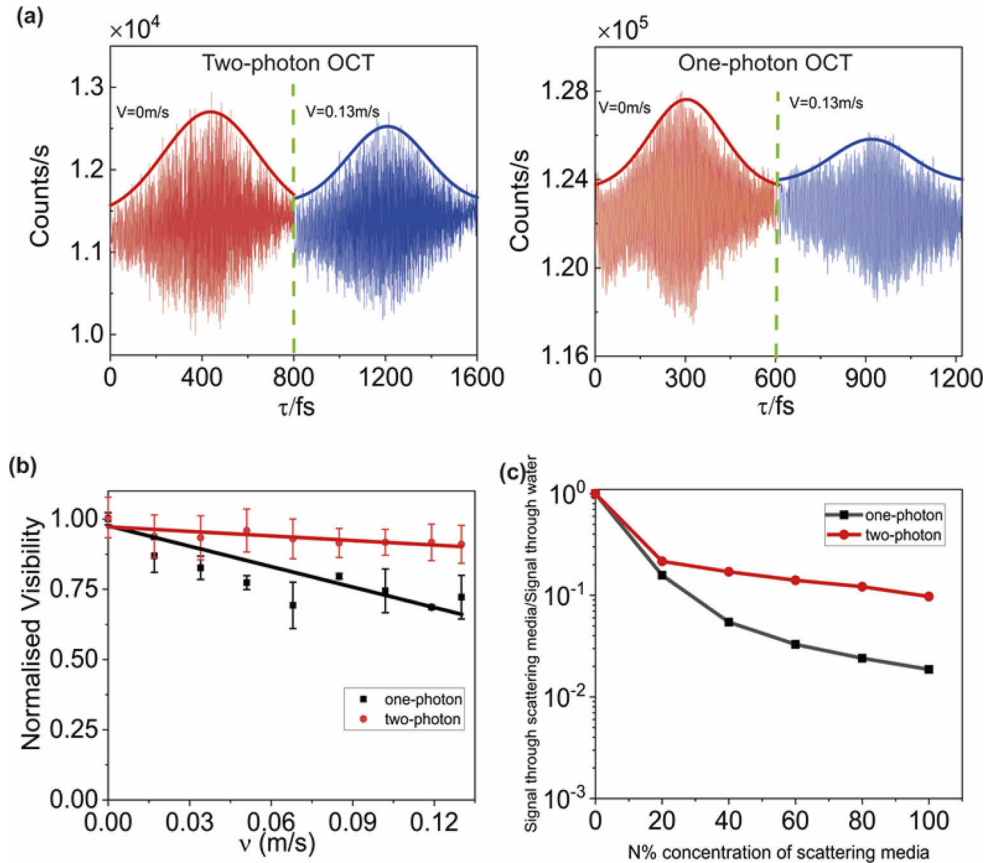


Fig. 3. Comparison of the performances of one-photon and two-photon OCTs through dynamical scattering media. (a) Autocorrelation of the one-photon and two-photon signal photocounts during the stationary and the flowing scattering media. (b) The normalized visibility of autocorrelation for both cases with increasing the flowing velocity of soymilk. (c) The signal of the two-photon and one-photon photocounts through different concentrations of soymilk.

3.2. Coherent TPA imaging through dynamical scattering media

For a proof-of-principle experiment, coherent imaging through a dynamical scattering media based on TPA can be realized in a similar Michelson interferometer setup in Fig. 2(a). The image of target is x-y dimensions whose area is $2.5\text{mm} \times 2.5\text{mm}$ as shown with the inset of Fig. 4(a). According to the results of Fig. 3, flowing scattering media has an influence on visibility. Especially, the influence is shown clearly by autocorrelation. 2D scanned x-z cross-sections where x scanning is along x direction of target and z scanning represents original autocorrelation curves selecting the ballistic photons can vividly reveal the hidden object (Fig. 4(a)) behind a strong scattering layer. Here the scattering layer of thickness ~ 2 mm is measured to be 28 (14 for the single-pass) times mean-free-path for 632.8nm laser using according to Beer's law, comparable or even better to other state-of-art scattering imaging techniques like Refs.[16] and [29]. However,

two-photon processes allow accessing longer wavelengths for deeper penetration [21,22], thus the scattering layer of thickness ~ 2 mm is measured to be around 8 times mean-free-path for 1550 nm laser. Spatial imaging resolution is estimated to be around $50 \mu\text{m}$, which is determined by the numerical aperture of the lens system and the SNR of TPA. In the meantime, the axial resolution along the depth is around $75 \mu\text{m}$ ($\sim 500\text{fs}$) (Fig. 4(b)), which is inversely proportional to the bandwidth of laser source (EDFA) ~ 30 nm. Such an illumination source provides $\sim 500\text{fs}$ time gate, good enough to filter out ballistic components from the diffusion background with an acceptable SNR. Similar to a one-photon OCT case, a broader bandwidth light source, e.g. supercontinuum source, can be used for a better temporal resolution, i.e. axial resolution.

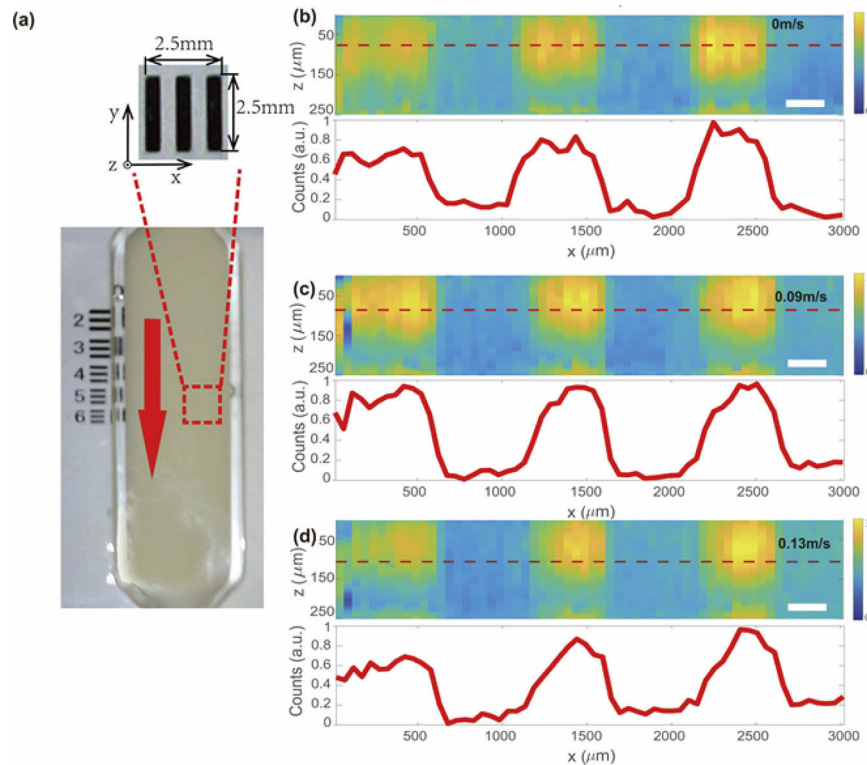


Fig. 4. Imaging through dynamic scattering media. (a) Image of target behind a running soymilk cuvette. Inset is the image of target. (b) Two-dimensional images of target (top) and their cross-sections along red dash line (bottom) behind the soymilk with the velocity of 0 m/s (b), 0.09 m/s (c) and 0.13 m/s (d). Color bar indicates signal intensity. The scale bar is $250 \mu\text{m}$

More importantly, Fig. 4(b)-(d) reveals the most significant feature of the current imaging method in dynamical scattering imaging. When the soymilk gradually increases its flow velocity from 0 to 0.13 m/s, the current method can still retrieve the target information despite the scatters' motion without losing too much SNR in Fig. 3(b). Ideally, scatters' moving speed is much slower compared to the light speed, hardly disturbing those ballistic photons. This lays the foundation for any ballistic imaging. However, in reality, the TPA detector has to integrate photon counts over a certain period in the millisecond scale. During this time, the ballistic light can be modulated by the moving scatters, hence, reducing the average signal counts. Especially, this effect is more pronounced near the boundary between "black" and "white" (for weak and strong reflection) regions as shown in Fig. 4(b)-(d). Nevertheless, the main features can still be resolved while

the problem caused by moving scatters can be solved with a faster and higher quantum-efficient semiconductor detector.

4. Discussion and conclusion

4.1. Imaging SNR analysis

The signal-to-noise ratio (SNR) is a main parameter which determines the performance of an OCT setup. The SNRs of one-photon OCT and two-photon OCT [30] are written:

$$\text{SNR}_{\text{one-photon}} = \sqrt{\frac{\gamma_{\text{one}} P_S R_S}{\hbar\omega B}} \quad (4)$$

$$\text{SNR}_{\text{two-photon}} = \frac{2\eta_{\text{TPA}}\gamma_{\text{two}}P_S R_S}{\text{NEP}\sqrt{B}} \quad (5)$$

η_{TPA} is the TPA quantum efficiency, γ_{two} (γ_{one}) is the quantum efficiency of the one-photon OCT (two-photon OCT) detectors, $\hbar\omega$ is the energy of the scattered photons from the sample, B is the electronic detection bandwidth, NEP is the noise equivalent power of the two-photon detector, P_S (P_R) is the power impinging on the sample (reference mirror) and R_S (R_R) is the sample (reference mirror) reflectivity. In the current experiment, TPA conversion efficiency is 10 cm GW^{-1} , the quantum efficiency of PMT is 12%, NEP [31] is $10^{-18} \text{ W(Hz)}^{-1/2}$, power impinging on a sample is 100mW and detector bandwidth is 5MHz, we estimate the sensitivity of $S=103 \text{ dBm}$ according to Eq. (5).

Besides the main advantage of phase-insensitive detection, two-photon OCT possesses several other benefits regarding the SNR, which have also been discussed in Ref. [30]. Comparing SNRs for one-photon/two-photon scenarios in Eqs. (4)/(5), the number of signal photons required to achieve the same level of SNRs is N for one-photon OCT, while \sqrt{N} for two-photon OCT, indicating a better SNR for the two-photon case. This nonlinear signal dependence has also been justified in the previous section of effective pinhole coherent imaging. Ref. [30] using a nonlinear sum-frequency upconversion, instead of TPA, has also pointed to a similar conclusion. However, early-arriving photons which fast decline as the thickness of scattering media increases are valuable for scattering media, which is the same as one-photon imaging. Thus thickness of the scattering media is a key factor which limits TPA measurement.

4.2. TPA illumination sources

The choices for TPA illumination sources are various, similar to one-photon OCT, including broadband sources, e.g. chaotic ASE, supercontinuum, and ultrafast pulsed lasers. Each has its own advantages depending on imaging purposes. For example, the broadband nature of ASE or supercontinuum sources in the current study enables the axial resolution down to several micrometers, similar to one-photon OCT. Furthermore, compared with coherent pulsed lasers which require pre-dispersion compensators for dispersive optical elements like objective lenses [32] configurations associated with the broadband source for TPA coherent imaging are not demanding due to the fact of phase insensitivity. On the other hand, TPA inherently is a nonlinear process solely depending on the peak power of illumination sources to excite. For example, the peak power of a femtosecond laser (300fs, 80 MHz) is 10^5 times than the one of chaotic light at the same average power, as a result, the TPA signal of the femtosecond laser is 10^{10} times than the latter case. Besides, according to the aforementioned theory, the peak-to-background ratio of chaotic light [18] is 8:2, but the peak-to-background ratio of a coherent short pulse [25] is 8:1, which helps improve SNR. Obviously, an ultrafast pulsed laser can greatly enhance the SNR for our TPA coherent imaging, however, at the expense of axial resolution, but it may be beneficial to some applications like confocal TPA imaging which doesn't require a reference to construct the axial information.

4.3. Future development

As compared to other existing imaging techniques through scattering media, two-photon coherent imaging by TPA exhibits several advantages towards practical implementations. First, as an inherent time-gate imaging method, ballistic imaging based on TPA with a temporal resolution at the femtosecond level can be implemented straightforwardly only requiring traditional semiconductor detectors. In contrast, imaging by nonlinear Kerr gate with a theoretical limit around the femtosecond level [24] need the same level pump femtosecond laser which is costly. Moreover, TPA in a semiconductor detector can be extended to an array, e.g. CMOS sensor [19], this can dramatically improve the image acquisition speed which can not be competed with free-space methods like nonlinear Kerr gate. Second, imaging methods based on light propagations through scattering matrices including time-reversal reconstruction [33] and adaptive optical correction [11] highly rely on prior knowledge about the scattering matrices by time-consuming reconstruction processes, hence it is impractical for real-time dynamical scattering imaging, elsewhere ballistic scattering, we believe, can perform better in this aspect. At last, the memory effect based on optical correlations offers a convenient physical way to retrieve information through scattering media. However, one of pioneering works [14] in this framework requires fluoresce-dyes to assist the image reconstruction; other experiments are performed under the transmission manner, not the highly desired reflective mode [13]. As a comparison, our work can operate in a non-invasive reflective setup without help from additional probes.

For future developments, two major factors: imaging resolution and speed in the current proof-of-principle experiment can be emphasized for practical applications. So far, our images with $\sim 50 \mu\text{m}$'s resolution and ~ 10 mins' acquisition time can be improved mainly by detection scheme. The main problem involving the resolution is due to the crosstalk of background scattering light and the signal, especially near the boundary layers. This issue can be overcome by shortening the time gate (broader laser pulse spectrum or ultrashort pulse laser) such that more ballistic signals can be detected to improve SNR. For this purpose, we may merge a lock-in amplification process using an analog PMT instead of photon-counting PMT, allowing improving imaging SNR and reducing recording time. Meanwhile, a CCD image array constructed by semiconductors can also facilitate image acquisition without scanning. However, traditional image arrays are noisy with low SNR, but other techniques like Microchannel plate (MCP) or Electron Multiplying CCD (EMCCD), which are also based on semiconductor technology can greatly reduce dark current and provide a sensitive detection for TPA ballistic imaging without scanning.

In conclusion, we experimentally demonstrate non-invasive coherent imaging by TPA through moving scattering media, where nonlinear TPA can be applied as an ultrafast time gate to distinguish ballistic photons from their scattering background. Images can be formed either through static or dynamical scattering media using the technique. This new method paves a new way for scattering imaging in biomedical applications.

Funding. National Natural Science Foundation of China (92050113, 11304201, 11674228); National Key Research and Development Program of China (2017YFA0303700, 2016YFA0302500); Shanghai MEC Scientific Innovation Program (E00075); Shanghai Scientific Innovation Program (14JC1402900); Shanghai Scientific Innovation Program for International Collaboration (15220721400).

Disclosures. The authors declare no conflicts of interest

Data availability. Data underlying the results presented in this paper are not publicly available at this time but may be obtained from the authors upon reasonable request.

References

1. P. Sheng, *Introduction to wave scattering, localization and mesoscopic phenomena* (Springer, 2006).
2. C. Dunsby and P. M. W. French, "Techniques for depth-resolved imaging through turbid media including coherence-gated imaging," *J. Phys. D: Appl. Phys.* **36**(14), R207–R227 (2003).
3. M. Klemm, J. A. Leendertz, D. Gibbins, I. J. Craddock, A. Preece, and R. Benjamin, "Microwave radar-based breast cancer detection: Imaging in inhomogeneous breast phantoms," *Antennas Wirel. Propag. Lett.* **8**, 1349–1352 (2009).

4. M. Batzle and Z. Wang, "Seismic properties of pore fluids," *Geophysics* **57**(11), 1396–1408 (1992).
5. J. Billy, V. Josse, Z. Zuo, A. Bernard, B. Hambrecht, P. Lugan, D. Clément, L. Sanchez-Palencia, P. Bouyer, and A. Aspect, "Direct observation of Anderson localization of matter waves in a controlled disorder," *Nature* **453**(7197), 891–894 (2008).
6. S. Feng, C. Kane, P. A. Lee, and A. D. Stone, "Correlations and fluctuations of coherent wave transmission through disordered media," *Phys. Rev. Lett.* **61**(7), 834–837 (1988).
7. I. Freund, M. Rosenbluh, and S. Feng, "Memory effects in propagation of optical waves through disordered media," *Phys. Rev. Lett.* **61**(20), 2328–2331 (1988).
8. Z. Yaqoob, D. Psaltis, M. S. Feld, and C. Yang, "Optical phase conjugation for turbidity suppression in biological samples," *Nat. Photonics* **2**(2), 110–115 (2008).
9. A. Badon, D. Li, G. Lerosey, A. C. Boccara, M. Fink, and A. Aubry, "Smart optical coherence tomography for ultra-deep imaging through highly scattering media," *Sci. Adv.* **2**(11), e1600370 (2016).
10. O. Katz, E. Small, and Y. Silberberg, "Looking around corners and through thin turbid layers in real time with scattered incoherent light," *Nat. Photonics* **6**(8), 549–553 (2012).
11. A. P. Mosk, A. Lagendijk, G. Lerosey, and M. Fink, "Controlling waves in space and time for imaging and focusing in complex media," *Nat. Photonics* **6**(5), 283–292 (2012).
12. E. Edrei and G. Scarcelli, "Optical imaging through dynamic turbid media using the Fourier-domain shower-curtain effect," *Optica* **3**(1), 71–74 (2016).
13. O. Katz, P. Heidmann, M. Fink, and S. Gigan, "Non-invasive single-shot imaging through scattering layers and around corners via speckle correlations," *Nat. Photonics* **8**(10), 784–790 (2014).
14. J. Bertolotti, E. G. V. Putten, C. Blum, A. Lagendijk, W. L. Vos, and A. P. Mosk, "Non-invasive imaging through opaque scattering layers," *Nature* **491**(7423), 232–234 (2012).
15. L. Wang, P. P. Ho, C. Liu, G. Zhang, and R. R. Alfano, "Ballistic 2-D imaging through scattering walls using an ultrafast optical Kerr gate," *Science* **253**(5021), 769–771 (1991).
16. D. Huang, E. A. Swanson, C. P. Lin, J. S. Schuman, W. G. Stinson, W. Chang, M. R. Hee, T. Flotte, K. Gregory, C. A. Puliafito, and J. G. Fujimoto, "Optical coherence tomography," *Science* **254**(5035), 1178–1181 (1991).
17. L. M. E. Zavallos, S. K. Gayen, M. Alrubaiee, and R. R. Alfano, "Time-gated backscattered ballistic light imaging of objects in turbid water," *Appl. Phys. Lett.* **86**(1), 011115 (2005).
18. F. Boitier, A. Godard, E. Rosencher, and C. Fabre, "Measuring photon bunching at ultrashort timescale by two-photon absorption in semiconductors," *Nat. Phys.* **5**(4), 267–270 (2009).
19. D. Panasenko and Y. Fainman, "Single-shot sonogram generation for femtosecond laser pulse diagnostics by use of two-photon absorption in a silicon CCD camera," *Opt. Lett.* **27**(16), 1475–1477 (2002).
20. A. Nevet, T. Michaeli, and M. Orenstein, "Second-order optical coherence tomography: deeper and turbulence-free imaging," *J. Opt. Soc. Am. B* **30**(2), 258–265 (2013).
21. N. M. Israelsen, C. R. Petersen, A. Barh, D. Jain, M. Jensen, G. Hanneschläger, P. Tidemand-Lichtenberg, C. Pedersen, A. Podoleanu, and O. Bang, "Real-time high-resolution mid-infrared optical coherence tomography," *Light: Sci. Appl.* **8**(1), 11–13 (2019).
22. D. A. Fishman, C. M. Cirloganu, S. Webster, L. A. Padilha, M. Monroe, D. J. Hagan, and E. W. Van Stryland, "Sensitive mid-infrared detection in wide-bandgap semiconductors using extreme non-degenerate two-photon absorption," *Nat. Photonics* **5**(9), 561–565 (2011).
23. T. H. Ko, D. C. Adler, J. G. Fujimoto, D. Mamedov, V. Prokhorov, V. Shidlovski, and S. Yakubovich, "Ultrahigh resolution optical coherence tomography imaging with a broadband superluminescent diode light source," *Opt. Express* **12**(10), 2112–2119 (2004).
24. W. Tan, Z. Zhou, A. Lin, J. Si, P. Zhan, B. Wu, and X. Hou, "High contrast ballistic imaging using femtosecond optical Kerr gate of tellurite glass," *Opt. Express* **21**(6), 7740–7747 (2013).
25. J. M. Roth, T. E. Murphy, and C. Xu, "Ultrasensitive and high-dynamic-range two-photon absorption in a GaAs photomultiplier tube," *Opt. Lett.* **27**(23), 2076–2078 (2002).
26. R. Loudon, *The Quantum Theory of Light* (Oxford University 2000).
27. R. L. Smith, "Two-photon photoelectric effect," *Phys. Rev.* **128**(5), 2225–2229 (1962).
28. K. Mogi, K. Naganuma, and H. Yamada, "A novel real-time chirp measurement method for ultrashort optical pulses," *Jpn. J. Appl. Phys.* **27**(Part 1, No. 11), 2078–2081 (1988).
29. J. A. Izatt, M. R. Hee, G. M. Owen, E. A. Swanson, and J. G. Fujimoto, "Optical coherence microscopy in scattering media," *Opt. Lett.* **19**(8), 590–592 (1994).
30. A. Pe'er, Y. Bromberg, B. Dayan, Y. Silberberg, and A. A. Friesem, "Broadband sum-frequency generation as an efficient two-photon detector for optical tomography," *Opt. Express* **15**(14), 8760–8769 (2007).
31. M. Akiba, K. Tsujino, and M. Sasaki, "Ultrahigh-sensitivity single-photon detection with linear-mode silicon avalanche photodiode," *Opt. Lett.* **35**(15), 2621–2623 (2010).
32. Y. Jiang, I. Tomov, Y. Wang, and Z. Chen, "Second-harmonic optical coherence tomography," *Opt. Lett.* **29**(10), 1090–1092 (2004).
33. X. Xu, H. Liu, and L. V. Wang, "Time-reversed ultrasonically encoded optical focusing into scattering media," *Nat. Photonics* **5**(3), 154–157 (2011).